

## Research Article

## Numerical Study and Optimization of the Thermomechanical Procedure in Forging of Two-Phase Ti-6Al-4V Alloy for Artificial Hip Joint Implant

H. Gheshlaghi<sup>1</sup>, V. Alimirzaloo<sup>1</sup>, M. Shahbaz<sup>2\*</sup> and A. Amiri<sup>3</sup>

<sup>1</sup> Department of Mechanical Engineering, Faculty of Engineering, Urmia University, Urmia, 15311-57561, Iran

<sup>2</sup> Department of Materials Science and Engineering, Faculty of Engineering, Urmia University, Urmia, 15311-57561, Iran

<sup>3</sup> Mechanical Engineering Department, Islamic Azad University, North Tehran Branch, Tehran, Iran

## ARTICLE INFO

*Article history:*

Received 15 March 2022

Reviewed 14 April 2022

Revised 1 May 2022

Accepted 10 May 2022

*Keywords:*

Artificial hip joint

Finite element analysis

Ti-6Al-4V

Forging

Response surface methodology

## ABSTRACT

A multi-objective numerical optimization was used to study the forging process of a Ti-6Al-4V alloy in producing an artificial hip joint implant. The forging temperature was chosen in the Alpha-Beta two phase region around 900°C. In order to implement the numerical simulation, the Deform 3D commercial code was used. Response surface methodology (RSM) was considered and experiments based on various widths ( $w$ ), thickness of flash ( $t$ ), and billet diameter ( $d$ ) were designed to find out the influences of these parameters on flash volume, filling rate and strain non-uniformity as the responses. Twenty numerical tests were implemented by finite element analysis (FEA), and the obtained results were used to optimize the forging process using RSM. To this end, the constants of constitutive and governing equations to FEA and the data of a published paper were applied. The optimized results were  $w = 8$  mm,  $t = 1.73$  mm, and  $d = 30$  mm, for flash geometry and billet diameter, respectively. Finally, an FEA was conducted based on the optimized values, and the results were compared and discussed with those in the Noiyberg-Mokel model for verification.

© Shiraz University, Shiraz, Iran, 2022

### 1. Introduction

Due to the excellent properties of Ti-6Al-4V, its compatibility with body tissue [1], lack of toxic ions, elasticity module near the bone elasticity, and perfect fatigue life [2], it is considered as the first choice in load-bearing implants such as manufacturing of artificial hip joints, dental implants, and other surgical implants [3-5]. On the other hand, due to the vast demand for artificial implants in the medical industry, hip joints from Ti-6Al-4V are promptly increasing, and many investigations

have been carried out in this regard [6-10]. Some methods such as forging, casting, and machining have been applied for fabricating the artificial hip joints. However, due to the higher strength, the ability to produce geometrically complicated parts, resistance to impact, lack of defects, strength in the desired direction and low porosity, the hot forging process can be considered as an effective method to manufacture artificial hip joints [11]. Parameters of the forging processes such as the geometry of die and billet diameter can considerably affect the outcome of its mechanical

\* Corresponding author

E-mail address: [m.shahbaz@urmia.ac.ir](mailto:m.shahbaz@urmia.ac.ir) (M. Shahbaz)

<https://doi.org/10.22099/IJMF.2022.43334.1219>

characteristics. Thus, the evaluation of the relations between input and output variables has a crucial role in the effectiveness of the mentioned process. On the other hand, Ti-6Al-4V is a two-phase alloy consisting of  $\alpha$  and  $\beta$  phases at room temperature, which can achieve varieties of properties by changing their characteristics. The mechanical properties of this material strongly depend on the initial condition of the as-received material and processing parameters. Due to the lack of sufficient study in the field of die design and optimization study in forging of the hip joint implant, some other related forging processes are presented to show the effectiveness of the optimization die methods in the forging processes.

Richard Turner et al. [12] investigated the forging process of a multi-partitioned titanium alloy billet for a medical implant by utilizing the 3D FEM method. They established a coupled thermal and mechanical procedure via applying the commercial Deform software. Four models were developed containing various arrangements of partitioning the initial billet with different titanium alloys assigned to partitions. Finally, one partition combination showed a very unsuccessful filling of the forging die, while the others filled the die and delivered various partitions maintained at the critical component locations. Torabi et al. [13] applied response surface methodology (RSM) and NSGA II to study the effects of forging parameters of an extruded elliptical cross-section of Ti-6Al-4V alloy on the minimum flash volume, maximum filling ratio of the final die, forging load and strain variance of the final product. Results, verified by the physical modeling method, depicted that the optimized preform shows better results than the conventional method. Jun Cai et al. [14] used a 3D electrostatic geometric transformation and field simulation to develop a new method to perform the design. Two axisymmetric forgings parts with a long-axis were used to demonstrate the performance of this method, and the Deform-3D software was also used to verify the validity and effectiveness of this approach. Alimirzaloo et al. [15] formulated and optimized the objective functions of the forging of Ti-6Al-4V using a genetic algorithm, finite element method, and RSM.

Results showed a good agreement between the numerical results and experimental tests.

This study investigates a thermomechanical model to be applied to simulate the forging of artificial hip joints for two-phase Ti-6Al-4V alloy. Due to the importance of the flash geometry and billet diameter, as shown in Fig. 1, on the hot-forged hip joints from Ti-6Al-4V, strain distribution, filling rate, and flash volume need to be investigated considerably. Moreover, it was found that the former studies have not focused on die design and optimization of the Ti-6Al-4V hip joint forging. Therefore, because of this gap, the commercial finite element software Deform-3D, was selected to simulate this hot forging process. The lack of sufficient equipment and the high cost of fabricating forging die, made the manufacturing and implementation of the designed forge die difficult. Hence, in order to verify the validity of the used numerical procedure, the current simulation procedure was firstly verified by work done in a published paper [16]. The design of the experiment and RSM was selected to investigate and optimize the effect of width ( $w$ ) and thickness of flash ( $t$ ) and billet diameter ( $d$ ) on flash volume, filling rate, and strain uniformity.

## 2. Finite Element Analysis

The accuracy of current finite element analyses (FEA) in the case of using materials behavior was verified by conducting a simulation of work done in reference [16]. For this purpose, the constants used for simulation were the same as those in the above-mentioned reference (Table 1). In the next step, the thermomechanical procedure

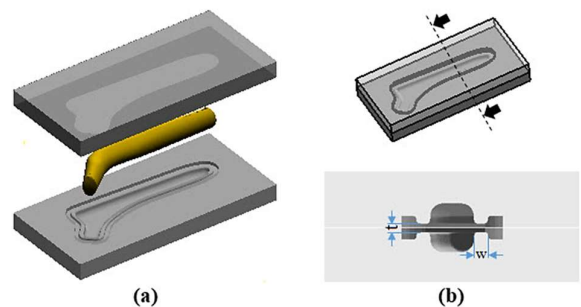


Fig. 1. (a) Hip joint forging die, and (b) geometry of the flash area on the hip joint die.

considered for simulations of the hot forging of the hip joint (Fig. 2) was simulated based on the same material behavior as used in the reference [16]. As can be seen, firstly, the alloy temperature was raised to 900°C in 15 min, followed by the workpiece being transferred from the inside of the furnace to the bending mold in 10 s. Subsequently, the bending process was performed, then the workpiece was brought to a temperature of 900°C, and after being transferred from the furnace to the forging mold (pre-heated to 400°C) for 10 s, the forging operation was performed with the speed of 80 mm/s. Finally, the forged samples were air-cooled. The physical-thermal parameters, including thermal

conductivity and heat capacity of Ti-6Al-4V, heat transfer coefficient at workpiece/die interface, and air convection coefficient were considered to be 6.6 W/m °C, 565 J/kg °C, 5 N/s/mm/°C, and 0.02.

Effective design of the forging die depends on several parameters, such as the parting line between two parts of the die, the final cavity of the die, and flash design. The parting line was considered in the middle of the die, which divides the die section into two equal parts. This can facilitate material uniform flow and easy machining in operation. The design of the final die cavity was developed based on dimensional considerations. Implementation of these dimensional considerations plays an essential role in the final quality of the fabricated part. Some of these parameters can be listed as follows: more machining chips, shrinkage, die wear, and slope. In the optimal forge die design, 0.08 of initial volume as extra thickness, and 7° as a slope angle for dying vertical surface were allocated [17]. Flash channel was considered on the die surfaces to accumulate extra material from the die gate. The geometry of the flash should be able to pass material without any resistance against the material flow. There are various methods to design flash channels and gates. These include the Noiyberg-Mokel [17] model and the Berachonov-Rebbsky [17] model. In most of these models, the final formula is presented in terms of the complexity of the piece's shape and its mass. The Noiyberg-Mokel model is based on studies on forged parts and agrees with experimental observations. The Norberg and Mokel model was considered to design the flash channel in this paper. Based on Eqs. (1) and (2) [17], thickness and width of the flash channel were obtained, respectively, which is coincident with values achieved by Berachonov and Rebbsky's relation.

**Table 1.** Constants for verification simulations of work done in the reference [16]

| Parameter   | Value |
|---|-------|
| Friction factor   | 0.7   |
| Heat transfer coefficient between workpiece and die (N/s/mm/°C) | 5     |
| Environment temperature (°C)                                    | 20    |
| Ram velocity (mm/s)   | 550   |
| Convection coefficient to environment (N/s mm/°C)               | 0.02  |
| Thermal conductivity (W/m °C)                                   | 6.6   |
| Heat capacity (J/kg °C)   | 565   |
| Emissivity  | 0.7   |
| Poisson's ratio   | 0.31  |
| Density (g/cm <sup>3</sup> )                                    | 4.43  |
| Die temperature (°C)  | 180   |
| Initial workpiece temperature (°C)                              | 980   |

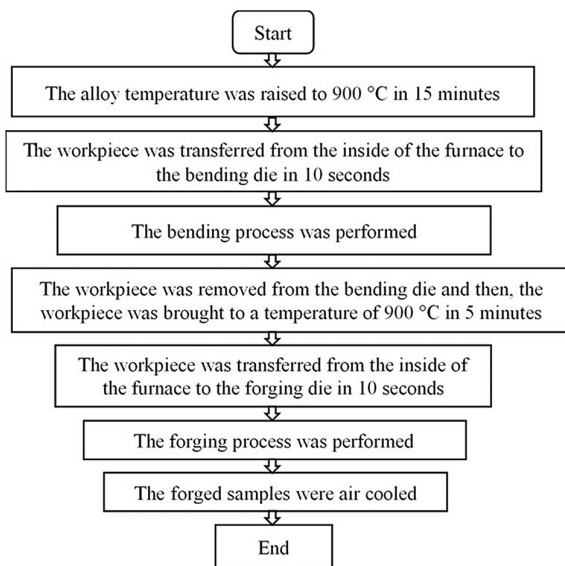


**Fig. 2.** The thermomechanical procedure used in this study.

$$t = 1.13 + 0.89\sqrt{m_w} - 0.017m_w \quad (1)$$

$$\frac{w}{t} = 1.25e^{(-1.09m_w)} + 3 \quad (2)$$

where  $t$ ,  $w$  and  $m_w$  are the width and the thickness of the flash, and the mass of the forged sample without a flash, respectively.

Finally, Solid Works software [18] was used to design the die models purposed by the design of experiments (Table 2). The final die model (Fig. 1) was obtained from the final part (which consists of a model obtained from the coordinate measuring machine (CMM) by adding some dimensional considerations such as total thickness). In a later stage, initial bending and forging dies were modeled based on the forge desirable part model. In the die design for titanium alloys, hot-worked H13 with a hardness range of 47-55 RC was applied. Because of the higher hardness of the dies in this analysis, dies were considered as discrete-rigid bodies. Fig. 3 shows the actual part and the final part of the model.

Tetrahedral elements, with the number of 75000 based on the mesh convergence criterion, were used to mesh the sample. To avoid any possible mesh distortion, automatic re-meshing was applied to all simulations.

To consider the frictional conditions similar to using glass tape as a lubricant between the die and the material, the shear friction model was selected with a constant friction factor of 0.3 in simulations [19].

### 3. Response Surface Methodology

In this study, for generating an RSM table using Design-Expert software V.11 [20], a central composite design in the form of a face centered ( $\alpha = 1$ ) with three factors, each in three levels ( $-1, 0, +1$ ) was used which resulted in 20 experimental conditions with six central points (Table 2).

In the forge die design, the optimum value of the flash volume, filling rate, and strain non-uniformity must be taken into consideration. To this end, the objective functions were defined as follows:



Fig. 3. (a) Actual part (b) final part model.

Table 2. Parameters, their levels and responses of the designed experiments for the forging of Ti-6Al-4V alloy

| Run | Input parameters             |                          |                               | Responses                             |                     |                                |
|-----|------------------------------|--------------------------|-------------------------------|---------------------------------------|---------------------|--------------------------------|
|     | A: Flash thickness, $t$ (mm) | B: Flash width, $w$ (mm) | C: Initial diameter, $d$ (mm) | Flash volume, $F.V$ ( $\text{mm}^3$ ) | Filling rate, $F.R$ | Strain non-uniformity, $S.N.U$ |
| 1   | 1.0                          | 3.0                      | 25.0                          | 81.90                                 | 0.932               | 0.0011                         |
| 2   | 2.4                          | 3.0                      | 25.0                          | 87.21                                 | 0.883               | 0.0011                         |
| 3   | 1.0                          | 10.0                     | 25.0                          | 85.41                                 | 0.910               | 0.0008                         |
| 4   | 2.4                          | 10.0                     | 25.0                          | 82.52                                 | 0.905               | 0.0007                         |
| 5   | 1.0                          | 3.0                      | 30.0                          | 226.31                                | 0.972               | 0.0023                         |
| 6   | 2.4                          | 3.0                      | 30.0                          | 243.76                                | 0.943               | 0.0026                         |
| 7   | 1.0                          | 10.0                     | 30.0                          | 222.18                                | 0.978               | 0.0028                         |
| 8   | 2.4                          | 10.0                     | 30.0                          | 233.83                                | 0.994               | 0.0032                         |
| 9   | 1.0                          | 6.5                      | 27.5                          | 162.99                                | 0.972               | 0.0019                         |
| 10  | 2.4                          | 6.5                      | 27.5                          | 176.89                                | 0.961               | 0.0020                         |
| 11  | 1.7                          | 3.0                      | 27.5                          | 170.65                                | 0.963               | 0.0020                         |
| 12  | 1.7                          | 10.0                     | 27.5                          | 160.57                                | 0.970               | 0.0021                         |
| 13  | 1.7                          | 6.5                      | 25.0                          | 62.08                                 | 0.923               | 0.0005                         |
| 14  | 1.7                          | 6.5                      | 30.0                          | 211.73                                | 1                   | 0.0023                         |
| 15  | 1.7                          | 6.5                      | 27.5                          | 156.64                                | 0.979               | 0.0018                         |
| 16  | 1.7                          | 6.5                      | 27.5                          | 156.64                                | 0.979               | 0.0018                         |
| 17  | 1.7                          | 6.5                      | 27.5                          | 156.64                                | 0.979               | 0.0018                         |
| 18  | 1.7                          | 6.5                      | 27.5                          | 156.64                                | 0.979               | 0.0018                         |
| 19  | 1.7                          | 6.5                      | 27.5                          | 156.64                                | 0.979               | 0.0018                         |
| 20  | 1.7                          | 6.5                      | 27.5                          | 156.64                                | 0.979               | 0.0018                         |

- Die filling was considered as one of the objectives of optimization using Eq. (3) [21]:

$$F.R = \frac{v_{desire}}{v_{actual}} \quad (3)$$

where  $v_{desire}$  is the desired volume (volume of the desired final part without flash), and  $v_{actual}$  is the volume of the actual final part after trimming the flash.

- Objective function for strain non-uniformity was defined as Eq. (4) [13]:

$$S.N.U = \frac{\sum_{i=1}^n |\bar{E}_i - \bar{E}_{ave}|}{n} \quad (4)$$

where  $\bar{E}_i$  and  $\bar{E}_{ave}$  are  $i^{\text{th}}$  element strain and elements average strain, respectively.

- Flash volume is obtained by Eq. (5), as follows [13]:

$$F.V = v_{fp} - v_{actual} \quad (5)$$

where  $v_{fp}$  and  $v_{actual}$  are the volumes of the final forging before and after trimming flash, respectively.

Analysis of variance (ANOVA) was considered to study the significance of input parameters based on the F- and p-value. Higher F-values indicate the higher the relative variance among the group [22]. The predetermined significance level of 0.05 (by default) was selected for the p-value, which values lower than it for the model and parameters indicate the significance of each [22].

#### 4. Results and Discussion

In order to perform a comparative evaluation, the processing load and temperature distribution over operation were inspected, and the results were depicted in Fig. 4 and Fig. 5. Fig. 4 shows the forging load vs. time for the results obtained in reference [16] and finite element analysis (FEA) of the current work. As depicted, for both cases, the diagram welcomes a steady upward trend until about 0.03 s with the value of 50 tons. However, a sharp increase is obtained for the rest of the

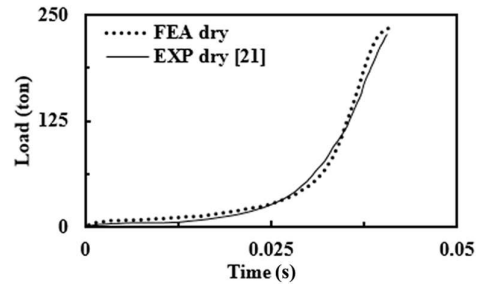


Fig. 4. Experimental and numerical load curves result for the tested conditions.

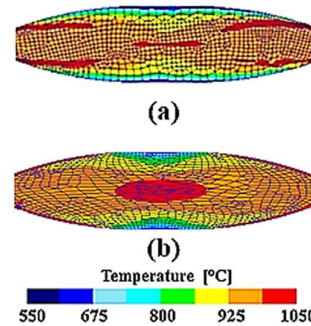


Fig. 5. Temperature distribution obtained by numerical simulation, (a) reference [16], and (b) current study.

period reaching the final value of 230 tons. It is noteworthy that, the trend of the load variations is almost the same, although, due to the simplification of the numerical method, some deviations were seen between their results, reaching the maximum value of 4.3% at the final step. Fig. 5 represents temperature distribution for the results obtained in reference [16] and FEA of the current work. Temperature domain were limited to 550-1050°C with a maximum value of 1050°C at the center of the billet for both cases. However, as it moves to surface layers, a smoother and lower temperature distribution is achieved. Moreover, although, at side areas near flash gates, the temperature value lowers with respect to central parts, in comparison with surface layers, it owns higher values. Based on the performed comparative study between the current numerical model and works done in reference [16], it was seen that the current numerical model has an acceptable precision, and hence, its results and outcomes can be applied for the implementation of paper purposes.

Tables 3, 4, and 5 show the ANOVA results for filling rate, flash volume, and strain non-uniformity

**Table 3.** ANOVA results for the filling rate response

| Source                            | Sum of squares | df                            | Mean square | F-value                        | p-value  |             |                 |
|-----------------------------------|----------------|-------------------------------|-------------|--------------------------------|----------|-------------|-----------------|
| Model                             | 0.0194         | 9                             | 0.0022      | 226.36                         | < 0.0001 | significant |                 |
| A: Flash thickness ( $t$ )        | 0.0006         | 1                             | 0.0006      | 60.98                          | < 0.0001 |             |                 |
| B: Flash width ( $w$ )            | 0.0004         | 1                             | 0.0004      | 41.42                          | < 0.0001 |             |                 |
| C: Initial diameter ( $d$ )       | 0.0111         | 1                             | 0.0111      | 1163.79                        | < 0.0001 |             |                 |
| AB: ( $t \times w$ )              | 0.0010         | 1                             | 0.0010      | 104.91                         | < 0.0001 |             |                 |
| AC: ( $t \times d$ )              | 0.0002         | 1                             | 0.0002      | 20.79                          | 0.0010   |             |                 |
| BC: ( $w \times d$ )              | 0.0004         | 1                             | 0.0004      | 45.08                          | < 0.0001 |             |                 |
| A <sup>2</sup> : ( $t \times t$ ) | 0.0003         | 1                             | 0.0003      | 36.67                          | 0.0001   |             |                 |
| B <sup>2</sup> : ( $w \times w$ ) | 0.0004         | 1                             | 0.0004      | 37.98                          | 0.0001   |             |                 |
| C <sup>2</sup> : ( $d \times d$ ) | 0.0008         | 1                             | 0.0008      | 79.75                          | < 0.0001 |             |                 |
| Residual                          | 8.333E-07      | 10                            | 8.333E-8    |                                |          |             |                 |
| Lack of fit                       | 5.687E-07      | 5                             | 1.1374E-7   |                                |          |             | not significant |
| Pure error                        | 2.646E-07      | 5                             | 5.292E-8    |                                |          |             |                 |
| R <sup>2</sup> = 99.48%           |                | R <sup>2</sup> (adj) = 99.01% |             | R <sup>2</sup> (pred) = 96.01% |          |             |                 |

**Table 4.** ANOVA results for the flash volume response

| Source                            | Sum of squares | df                            | Mean square | F-value                        | p-value  |             |                 |
|-----------------------------------|----------------|-------------------------------|-------------|--------------------------------|----------|-------------|-----------------|
| Model                             | 56265.00       | 9                             | 6251.67     | 1839.61                        | < 0.0001 | significant |                 |
| A: Flash thickness ( $t$ )        | 206.30         | 1                             | 206.30      | 60.71                          | < 0.0001 |             |                 |
| B: Flash width ( $w$ )            | 64.11          | 1                             | 64.11       | 18.87                          | 0.0015   |             |                 |
| C: Initial diameter ( $d$ )       | 54566.29       | 1                             | 54566.29    | 16056.65                       | < 0.0001 |             |                 |
| AB: ( $t \times w$ )              | 24.50          | 1                             | 24.50       | 7.21                           | 0.0229   |             |                 |
| AC: ( $t \times D$ )              | 88.98          | 1                             | 88.98       | 26.18                          | 0.0005   |             |                 |
| BC: ( $w \times D$ )              | 20.74          | 1                             | 20.74       | 6.10                           | 0.0331   |             |                 |
| A <sup>2</sup> : ( $t \times t$ ) | 452.92         | 1                             | 452.92      | 133.27                         | < 0.0001 |             |                 |
| B <sup>2</sup> : ( $w \times w$ ) | 198.85         | 1                             | 198.85      | 58.51                          | < 0.0001 |             |                 |
| C <sup>2</sup> : ( $d \times d$ ) | 1122.29        | 1                             | 1122.29     | 330.24                         | < 0.0001 |             |                 |
| Residual                          | 4.98           | 10                            | 0.498       |                                |          |             |                 |
| Lack of fit                       | 3.12           | 5                             | 0.624       |                                |          |             | not significant |
| Pure error                        | 1.86           | 5                             | 0.372       |                                |          |             |                 |
| R <sup>2</sup> = 99.94%           |                | R <sup>2</sup> (adj) = 99.89% |             | R <sup>2</sup> (pred) = 99.52% |          |             |                 |

**Table 5.** ANOVA results for the strain non-uniformity response

| Source                            | Sum of squares | df                            | Mean square | F-value                        | p-value  |             |                 |
|-----------------------------------|----------------|-------------------------------|-------------|--------------------------------|----------|-------------|-----------------|
| Model                             | 9.421E-06      | 9                             | 1.047E-06   | 1214.66                        | < 0.0001 | significant |                 |
| A: Flash thickness ( $t$ )        | 5.592E-08      | 1                             | 5.592E-08   | 64.89                          | < 0.0001 |             |                 |
| B: Flash width ( $w$ )            | 2.041E-08      | 1                             | 2.041E-08   | 23.69                          | 0.0007   |             |                 |
| C: Initial diameter ( $d$ )       | 8.219E-06      | 1                             | 8.219E-06   | 9537.39                        | < 0.0001 |             |                 |
| AB: ( $t \times w$ )              | 1.445E-10      | 1                             | 1.445E-10   | 0.1677                         | 0.6908   |             |                 |
| AC: ( $t \times d$ )              | 8.740E-08      | 1                             | 8.740E-08   | 101.42                         | < 0.0001 |             |                 |
| BC: ( $w \times d$ )              | 5.023E-07      | 1                             | 5.023E-07   | 582.86                         | < 0.0001 |             |                 |
| A <sup>2</sup> : ( $t \times t$ ) | 6.346E-08      | 1                             | 6.346E-08   | 73.63                          | < 0.0001 |             |                 |
| B <sup>2</sup> : ( $w \times w$ ) | 1.776E-07      | 1                             | 1.776E-07   | 206.04                         | < 0.0001 |             |                 |
| C <sup>2</sup> : ( $d \times d$ ) | 4.941E-07      | 1                             | 4.941E-07   | 573.39                         | < 0.0001 |             |                 |
| Residual                          | 8.618E-09      | 10                            | 8.618E-10   |                                |          |             |                 |
| Lack of fit                       | 4.761E-09      | 5                             | 9.521E-10   |                                |          |             | not significant |
| Pure error                        | 3.857E-09      | 5                             | 7.715E-10   |                                |          |             |                 |
| R <sup>2</sup> = 99.91%           |                | R <sup>2</sup> (adj) = 99.83% |             | R <sup>2</sup> (pred) = 99.27% |          |             |                 |

within the forging product, respectively. As can be seen, the processing parameter of initial diameter ( $d$ ) has the most significant effect on the amount of filling rate, which seems reasonable given the type of process and the shaping area that exists between the molds. After that, flash thickness ( $t$ ) and flash width ( $w$ ) affect the responses, respectively.

According to Table 3, the processing parameters of initial diameter ( $d$ ), flash thickness ( $t$ ), and interactions of  $t \times w$  and  $d \times d$  are the most significant parameters affecting strain non-uniformity, while according to Table 4, the processing parameters of initial diameter ( $d$ ), flash thickness ( $t$ ) and the interactions of  $t \times d$ ,  $d \times d$ , and  $t \times t$  are the most significant parameters affecting the flash volume and as observed in Table 5, the processing parameters of initial diameter ( $d$ ), flash thickness ( $t$ ), and the interactions of  $w \times d$ ,  $t \times d$ ,  $d \times d$ , and  $w \times w$  are the most significant parameters affecting the strain non-uniformity.

RSM-based mathematical equations for filling rate, flash volume, and strain non-uniformity as a function of  $t$ ,  $w$ , and  $d$  as input parameters were developed. The determination coefficient  $R^2$ , adjusted determination coefficient (adjusted- $R^2$ ), predicted  $R^2$ , and prediction error sum of squares were used to check the models' adequacy. Comparison of mentioned factors for linear, two factors interaction (2FI), and quadratic models showed that, according to Tables 3, 4, and 5, the quadratic models (Eqs. (6), (7), and (8)) are more accurate for the regression analysis of filling rate, flash volume, and strain non-uniformity, respectively.

$$\begin{aligned} \text{Filling rate} = & +0.92 - 0.0076t - 0.0063w \\ & - 0.0333d + 0.0112(t \times w) \\ & + 0.005(t \times d) + 0.0073(w \times d) \\ & - 0.0113(t \times t) - 0.0115(w \times w) \\ & - 0.0166(d \times d) \end{aligned} \quad (6)$$

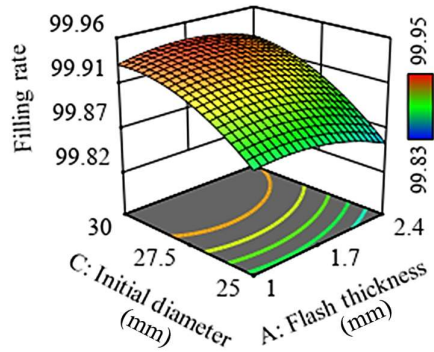
$$\begin{aligned} \text{Flash volume} = & +156.83 + 4.542t - 2.532w \\ & + 73.869d - 1.75(t \times w) \\ & + 3.335(t \times d) - 1.61(w \times d) \\ & + 12.8334(t \times t) + 8.5034(w \times w) \\ & + 20.2016(d \times d) \end{aligned} \quad (7)$$

$$\begin{aligned} \text{Strain non-uniformity} = & +0.0018 + 7.478 \times 10^{-5}t \\ & + 0.0000452w + 0.00091d \\ & - 0.00000425(t \times w) \\ & + 0.000104(t \times d) \\ & + 0.00025(w \times d) \\ & + 0.000152(t \times t) \\ & + 0.000254(w \times w) \\ & - 0.0004239(d \times d) \end{aligned} \quad (8)$$

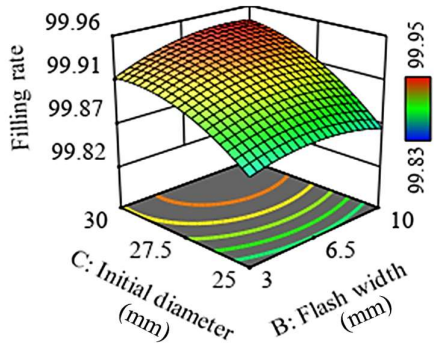
According to Fig. 6, by examining the effect of input parameters on the response variable of the die filling rate, it can be said that by increasing the thickness of the flash channel to 1.65 mm, the die filling rate increases. This increase is caused due to the reduction of material folding defects, strain hardening, and easy flow of materials. However, with an increase in thickness from 1.65 mm to 2.4 mm, the filling rate of the die significantly reduces (due to high friction, the material flows in a direction where the stress is low and exits the path of the flash channel). Additionally, by increasing the width of the flash channel to 7.1 mm, the filling of the die increased with a high slope, but a further rise in the width of the flash channel increases the load required for forging and strain hardening in the corners then reduces the filling of the die. Finally, by examining Fig. 6, it can be said that increasing the initial diameter, despite a rise in the amount of die filling, more flash is achieved.

As shown in Fig. 7, a 3D surface showing the main effect of the factors on the minimum amount of flash indicates that increasing the initial diameter of workpiece increases the amount of flashes. However, by increasing the thickness of the flash to the value of 1.65 mm, the amount of flash first decreases and then increases. The increase in the amount of flashes thicknesses higher than 1.65 mm is the more effortless flow of the material into the flash channel. It is noteworthy that in the experimental relationships for flash channel design, the values of channel thickness and width are related to each other. The dependence of these values for having the lowest amount of flash is also evident in the simulation results.

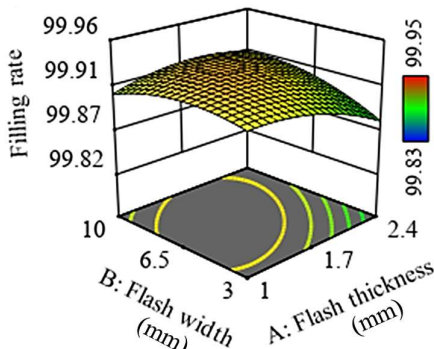
According to Fig. 8, by evaluating effects of the input variables on respond variables, it was seen that, there is



(a)



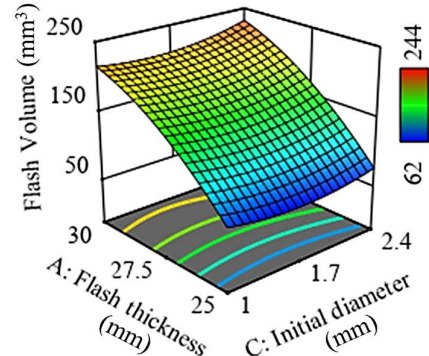
(b)



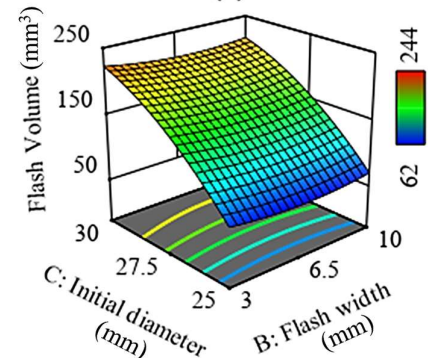
(c)

**Fig. 6.** Surface plots of filling rate for: (a) flash thickness and initial diameter ( $w = 6.5$  mm), (b) initial diameter and flash width ( $t = 1.7$  mm), and (c) flash width and flash thickness ( $d = 27.5$  mm).

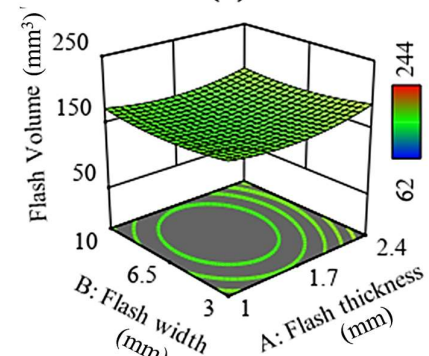
a considerable strain non-uniformity, which increases with bigger initial material diameter. Furthermore, a lack of prepared and accurate dimensions for thickness and width of the flash channel will cause more strain non-uniformity. Ultimately, it was released that, in values of 1.65 mm and 7.2 mm for thickness and width, respectively, the lowest non-uniformity was seen. Considerable effective strain values and an increase in the strain non-uniformity were seen for smaller sizes of



(a)



(b)

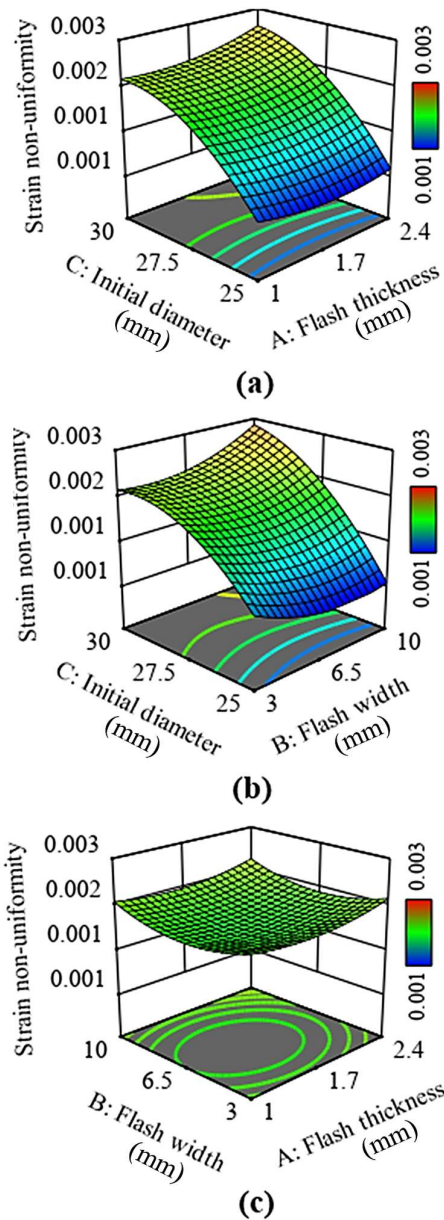


(c)

**Fig. 7.** Surface plots of flash volume for: (a) flash thickness and initial diameter ( $w = 6.5$  mm), (b) initial diameter and flash width ( $t = 1.7$  mm), and (c) flash width and flash thickness ( $d = 27.5$  mm).

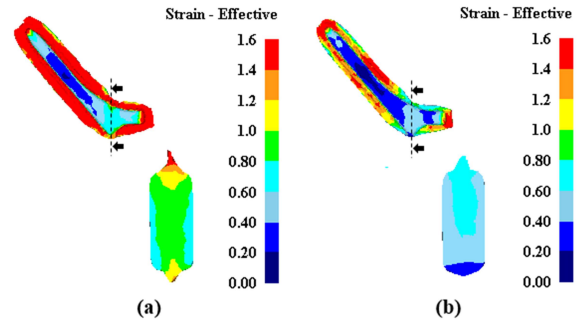
the flash channel thickness and width, which is due to the frictional condition and extra materials flow. Moreover, in bigger flash sizes, due to the lack of filling of die cavities, some sections are not filled accurately, which intensifies non-uniformity.

Fig. 9, depicts a comparative study for strain non-uniformity for the flash thickness of 1.7 mm and 1 mm on the section of the forged part (there is the possibility of fracture in this section) in the initial diameter of 30 mm



**Fig. 8.** Surface plots of strain non-uniformity for: (a) flash thickness and initial diameter ( $w = 6.5$  mm), (b) initial diameter and flash width ( $t = 1.7$  mm), and (c) flash width and flash thickness ( $d = 27.5$  mm).

and width of 10 mm. As can be seen, strain non-uniformity has mostly appeared around the flash area. Despite the improvement of strain uniformity in flash thickness of 1 mm, in die contact surface with part and inside the flash channel, due to the friction and higher temperatures, strain values increase and finally, non-uniformity percentage achieves higher values. In bigger flash sizes, some sections are not filled, and thus, non-uniformity rises. Under these circumstances, the filling



**Fig. 9.** Effective strain on section: (a) thickness of 1 mm, and (b) thickness of 1.7 mm.

rate reduces, and the final shape of the forged part will change. The higher and lower dimensions of flash thickness cause higher non-uniformity. Finally, in thickness of 1.7 mm and width of 6.5 mm, the lowest strain non-uniformity has appeared in the flash channel.

It is noteworthy to mention that, in the diameter of 30 mm, due to the higher volume of flash and its influences on the distribution of strains, the strain non-uniformity increases. If it is possible to diminish unnecessary material from the forged part, the strain non-uniformity will strongly decrease at 30 mm diameters, and the highest effective strain reaches 1.6 in the outer sections of the corners of the forged part.

Fig. 10, depicts a comparative study of the minimum distance between the workpiece and dies at the end of the forging process for the initial diameter of 27.5 mm and 30 mm in the flash thickness of 1.7 mm and width

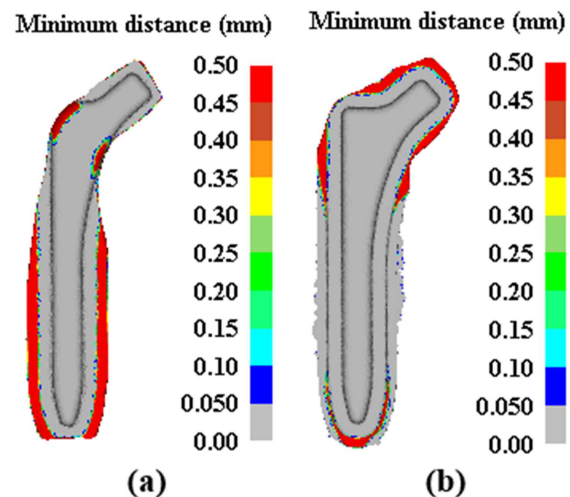


**Fig. 10.** The minimum distance between the workpiece and dies at the end of the forging: (a) the initial diameter of 27.5 mm, and (b) the initial diameter of 30 mm.

of 6.5 mm. As seen, in the initial diameter of 27.5 mm, there is a gap between the die and the workpiece. The minimum distance between the workpiece and the die mostly appears in the section shown in Fig. 10. By increasing the initial diameter to 30 mm, the die is filled, and at the same time, the amount of flashes increase.

As mentioned, the purpose of this paper is to optimize the multi-objective process of forging the hip joint process made of two-phase Ti-6Al-4V alloy by RSM method and the objective function in Design-Expert software. For this purpose, three input parameters, including initial diameter, thickness, and width of the flash and three output parameters, including strain non-uniformity, die filling, and flash volume, were considered as optimization variables. In the forging processes, the quality, and proper design of the fabricated part depends on the output parameters of the process. Therefore, during construction, the relationship between input and output parameters must be accurately identified and the ideal point must be achieved with proper process design. On the other hand, the effects of input variables on output variables are not uniform and constant, and increasing one input variable may improve one output variable, but at the same time weaken another. Therefore, by designing a proper multi-objective optimization, the effects of input variables on output variables can be optimized so that any change in input parameters will improve the overall output ones. For this purpose, before performing the optimization, it is necessary that the percentage of importance and ranking of the output parameters are selected based on the design requirements and applied in the software.

The relative importance of each response ( $r_i$ ) varies from the least important, a value of 1, to the most important, a value of 5, in the desirability objective function  $D(X)$  (Eq. (9)) [20]:

$$D = (d_1^{r_1} \cdot d_1^{r_2} \cdot \dots \cdot d_1^{r_n})^{\frac{1}{\sum r_i}} = \left( \prod_{i=1}^n d_i^{r_i} \right)^{\frac{1}{\sum r_i}} \quad (9)$$

where  $n$  is the number of responses in the measure and  $d_i$  is the individual desirability for each response. If all the important values are similar, the simultaneous

objective function reduces to the normal form for desirability.

It is also possible to use the “weight” field to change the shape of the desirability of each goal. With a weight of 1, the  $d_i$  will vary from 0 to 1 in a linear fashion. Weights more significant than 1 (maximum weight is 10), give more emphasis to the goal while weights less than 1 (minimum weight is 0.1), give less emphasis to the goal [20]. Table 6 shows the optimization parameters.

**Table 6.** The optimization parameters

|                       | goal     | Weights | Importance |
|-----------------------|----------|---------|------------|
| Filling rate          | Maximize | 10      | +++++      |
| Flash volume          | Minimize | 0.1     | +          |
| Strain non-uniformity | Minimize | 1       | +++        |

By considering the degree of desirability close to one (0.94), the desired values of flash, die filling rate, and strain uniformity were obtained by adjusting the channel thickness to 1.73 mm, the channel width to 8.05 mm, and the initial diameter of the workpiece to 30 mm (Fig. 11).

By designing the die models with obtained optimum dimensions and implementing numerical simulation with the optimum condition, flash volume, filling rate, and strain non-uniformity were calculated at 210.7 ( $\text{mm}^3$ ), 1.00 and 0.0025, respectively. These values correlate with optimized outputs and show the validity of the proposed model.

In most research works [18], Eqs. (1) and (2), known as the Noiyberg-Mokel model are used to calculate the dimensions of the flash channel. Based on the Noiyberg-Mokel model, considering a workpiece with an initial diameter of 30 mm, the thickness and width of the flash channel were 1.5 mm and 6.1 mm, respectively. By simulating the non-isothermal forging process based on

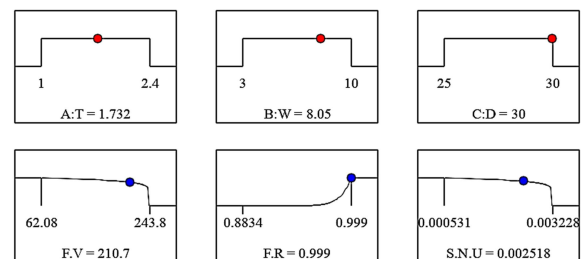


**Fig. 11.** Optimum values for input parameters.

the dimensions of the flash channel obtained from the Noiyberg-Mokel model the maximum amount of forging load and the amount of strain non-uniformity according to Fig. 12 and Fig. 13 were compared with the simulation results of the optimized dimension of the flash channel and its results are illustrated in Table 7. The results showed that in the flash channel with the optimized dimension, the maximum amount of forging load and the amount of strain non-uniformity is less than the simulation results done with the calculated dimensions of the Noiyberg-Mokel model (effective strain is also lower in the optimized conditions). Furthermore, according to Fig. 14, the minimum distance between the

**Table 7.** Simulation results with optimal dimensions and dimensions of Noiyberg-Mokel

|                                 | Optimal dimensions | Dimensions of Noiyberg-Mokel model |
|---------------------------------|--------------------|------------------------------------|
| Process load (tons)             | 579.9              | 665.6                              |
| Strain non-uniformity           | 0.0025             | 0.0033                             |
| Filling rate                    | 0.999              | 0.947                              |
| Flash volume (mm <sup>3</sup> ) | 210.7              | 233.8                              |

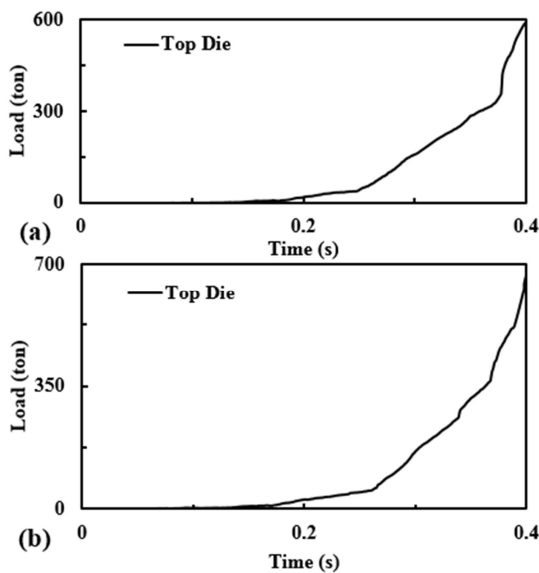


**Fig. 12.** Load-time curve for forging operation: (a) optimal dimensions, and (b) dimensions of Noiyberg-Mokel model.

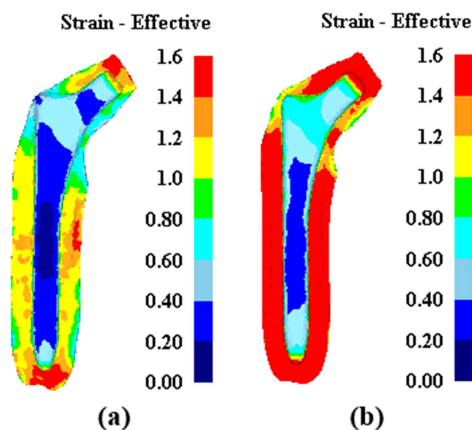


**Fig. 13.** Strain Effective at the end of the forging process: (a) optimal dimensions, and (b) dimensions of Noiyberg-Mokel model.

**Minimum distance (mm)**

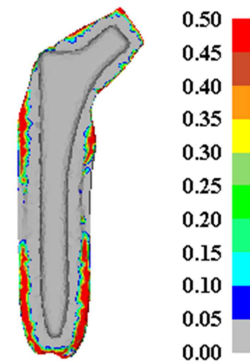


**Fig. 14.** The minimum distance between the workpiece and dies at the end of the forging process in the optimal dimensions.

workpiece and dies at the end of the forging process were displayed that depicted the fact that, the die is filled and the product is without any defect.

### 5. Conclusion

In this research, the design of the flash channel in the forging die of a hip joint implant made of Ti-6Al-4V alloy was investigated. The design of the dies was done in accordance with the design of the experiment approach performed by the response surface method. By analyzing the results and using the objective function, the dimensions of the flash channel and the initial diameter of billet were optimized. To evaluate the optimal point, it was necessary to numerically simulate this point using the finite element method and comparing the results with the outcomes obtained from numerical simulations based on the Noiyberg-Mokel model. By designing the dies with the obtained dimensions and performing the simulation, the results indicated that with the optimization method, the lowest flash volume and the highest filling rate and strain uniformity can be better

achieved in comparison with the results obtained from the use of the Noiyberg-Mokel model. Consequently; the accuracy of the model can be confirmed.

The following significant results were obtained:

- To achieve the minimum flash volume and strain non-uniformity, and the highest filling rate, the values of 8 mm, 1.73 mm, and 30 mm were obtained for the width and thickness of the flash channel and the initial diameter of the billet, respectively.
- By considering the degree of desirability close to one (0.94), the desired values of flash, die filling rate, and strain uniformity were obtained by adjusting the channel thickness to 1.73 mm, the channel width to 8.05 mm, and the initial diameter of the workpiece to 30 mm.
- By designing die models with obtained optimum dimensions and implementation of numerical simulation with the optimum condition, flash volume, filling rate, and strain non-uniformity were calculated at 210.7 (mm<sup>3</sup>), 1.00, and 0.0025, respectively.

### Funding

The work was financially supported by Urmia University, Urmia, Iran.

### Conflict of Interests

The authors declare that they have no conflict of interest.

### 6. References

- [1] M. Geetha, A.K. Singh, R. Asokamani, A.K. Gogia, Ti based biomaterials, the ultimate choice for orthopaedic implants—a review, *Progress in Materials Science*, 54(3) (2009) 397-425.
- [2] S.H. Teoh, Fatigue of biomaterials: a review, *International Journal of Fatigue*, 22(10) (2000) 825-837.
- [3] L.R. Saitova, H.W. Höppel, M. Göken, I.P. Semenova, G.I. Raab, R.Z. Valiev, Fatigue behavior of ultrafine-grained Ti-6Al-4V 'ELI' alloy for medical applications, *Materials Science and Engineering:A*, 503(1-2) (2009) 145-147.
- [4] R.K. Nalla, R.O. Ritchie, B.L. Boyce, J.P. Campbell, J.O. Peters, Influence of microstructure on high-cycle fatigue of Ti-6Al-4V: Bimodal vs. lamellar structures, *Metallurgical and Materials Transactions A*, 33(3) (2002) 899-918.
- [5] S. Bauer, P. Schmuki, K. Von Der Mark, J. Park, Engineering biocompatible implant surfaces: Part I: Materials and surfaces, *Progress in Materials Science*, 58(3) (2013) 261-326.
- [6] K. Čolić, A. Sedmak, K. Legweel, M. Milošević, N. Mitrović, Ž. Mišković, S. Hloch, Experimental and numerical research of mechanical behaviour of titanium alloy hip implant, *Tehnički vjesnik*, 24(3) (2017) 709-713.
- [7] K.S. Katti, Biomaterials in total joint replacement, *Colloids and Surfaces B: Biointerfaces*, 39(3) (2004) 133-42.
- [8] M. Balazic, J. Kopac, M.J. Jackson, W. Ahmed, Titanium and titanium alloy applications in medicine, *International Journal of Nano and Biomaterials*, 1(1) (2007) 3-34.
- [9] V.S. de Viteri, E. Fuentes, Titanium and titanium alloys as biomaterials, *Tribology-Fundamentals and Advancements*, 1(5) (2013) 154-181.
- [10] H.J. Rack, J.I. Qazi, Titanium alloys for biomedical applications, *Materials Science and Engineering: C*, 26(8) (2006) 1269-1277.
- [11] S.A. Shaik, K. Bose, H.P. Cherukuri, A study of durability of hip implants, *Materials & Design*, 42 (2012) 230-237.
- [12] R. Turner, J. Antonic, N. Warnken, 3D Forging simulation of a multi-partitioned titanium alloy billet for a medical implant, *Journal of Manufacturing and Materials Processing*, 3(3) (2019) 69.
- [13] S.H.R. Torabi, S. Alibabaei, B. Barooghi Bonab, M.H. Sadeghi, Gh. Faraji, Design and optimization of turbine blade perform forging using RSM and NSGA II, *Journal of Intelligent Manufacturing*, 28(6) (2017) 1409-1419.
- [14] J. Cai, F. Li, T. Liu, A new approach of preform design based on 3D electrostatic field simulation and geometric transformation" *The International Journal of Advanced Manufacturing Technology*, 56(5) (2011) 579-588.
- [15] V. Alimirzaloo, M.H. Sadeghi, F.R. Biglari, Optimization of the forging of aerofoil blade using the finite element method and fuzzy Pareto based genetic algorithm, *Journal of Mechanical Science and Technology*, 26(6) (2012) 1801-1810.
- [16] S. Bruschi, G. Buffa, A. Ducatoa, L. Fratini, A. Ghiotti, Phase evolution in hot forging of dual phase titanium alloys: Experiments and numerical analysis, *Journal of Manufacturing Processes*, 20 (2015) 382-388.

- [17] R. Sethy, L. Galdos, J. Mendiguren, E. Sáenz de Argandoña, Friction and heat transfer coefficient determination of titanium alloys during hot forging conditions, *Advanced Engineering Materials*, 19(6) (2017) 1600060.
- [18] V. Alimirzaloo, F.R. Biglari, M.H. Sadeghi, Numerical and experimental investigation of preform design for hot forging of an aerofoil blade, *Proceedings of the Institution of Mechanical Engineers, Part B: Journal of Engineering Manufacture*, 225(7) (2011) 1129-1139.
- [19] S.K. Choi, M.S. Chun, C.J. Van Tyne, Y.H. Moon, Optimization of open die forging of round shapes using FEM analysis, *Journal of Materials Processing Technology*, 172(1) (2006) 88-95.
- [20] D.C. Montgomery, Design and analysis of experiments, John Wiley & sons, 2017.
- [21] V. Ranatunga, J.S. Gunasekera, W.G. Frazierand, K.D. Hur, Use of UBET for design of flash gap in closed-die forging, *Journal of Materials Processing Technology*, 111(1-3) (2001) 107-112.
- [22] G. Ranjbari, A. Doniavi, M. Shahbaz, R. Ebrahimi, Effect of processing parameters on the strain inhomogeneity and processing load in vortex extrusion of Al–Mg–Si alloy, *Metals and Materials International*, 27(4) (2021) 683-690.